

DMD #37952

## Title page

### Title:

**Metabolism of the c-Fos/activator protein-1 inhibitor T-5224 by multiple human UGT isoforms**

### Authors:

Shinsuke Uchihashi

Hiroyuki Fukumoto

Makoto Onoda

Hiroyoshi Hayakawa

Shin-ichi Ikushiro

Toshiyuki Sakaki

Research Laboratories, Toyama Chemical Co., Ltd., 4-1, Shimookui, 2-Chome, Toyama, 930-8508, Japan (S.U., H.F., M.O. and H.H.)

Department of Biotechnology, Faculty of Engineering, Toyama Prefectural University, 5180 Kurokawa, Imizu, Toyama 939-0398, Japan (S.-i.I. and T.S.)

## Running title page

**Running title:** *In-Vitro* Glucuronidation of T-5224

### Address for correspondence:

Hiroyoshi Hayakawa

Drug Metabolism & Pharmacokinetics Department

Research Laboratories

Toyama Chemical Co., Ltd.

4-1, Shimookui, 2-Chome, Toyama, 930-8508, Japan

Tel: (+81) 76 431 8317

Fax: (+81) 76 431 8208

E-mail address: [hiroyoshi\\_hayakawa@toyama-chemical.co.jp](mailto:hiroyoshi_hayakawa@toyama-chemical.co.jp)

Pages: 39

Tables: 2

Figures: 9

References: 38

Words: Abstract; 229

Introduction; 337

Discussion; 1665

**Abbreviations:** human liver microsome (HLM), human intestinal microsome (HIM), UDP-glucuronosyltransferase (UGT), intrinsic clearance ( $CL_{int}$ ), cytochrome P450 (P450), UDP-glucuronic acid (UDPGA), dimethyl sulfoxide (DMSO), high-performance liquid chromatography (HPLC), HPLC/hybrid Fourier transform mass spectrometry (LC/hybrid FTMS), high-energy collision dissociation (HCD), coefficient variation (CV), nuclear magnetic resonance (NMR)

## **Abstract**

We developed T-5224 as a novel inhibitor of the c-Fos/activator protein-1 for rheumatoid arthritis therapy. We predicted the metabolism of T-5224 in humans by using human liver microsomes (HLMs), human intestinal microsomes (HIMs), recombinant human cytochrome P450 (P450) and UDP-glucuronosyltransferases (UGTs). T-5224 was converted to its acyl *O*-glucuronide (G2) by UGT1A1 and UGT1A3 and to its hydroxyl *O*-glucuronide (G3) by several UGTs, but it was not metabolized by the P450s. Comparing the intrinsic clearances ( $CL_{int}$ ) between HLM and HIM suggested that the glucuronidation of T-5224 predominantly occurs in the liver. UGT1A1 showed a higher  $k_{cat}/K_m$  value compared to UGT1A3 for the G2 formation but a lower  $k_{cat}/K_m$  value compared to UGT1A3 for G3 formation. A high correlation was observed between G2 formation activity and UGT1A1-specific activity ( $\beta$ -estradiol 3-glucuronidation) in 7 individual HLMs. A high correlation was also observed between G2 formation activity and UGT1A1 content in the HLMs. These results strongly suggest that UGT1A1 is responsible for the G2 formation in the human liver. In contrast, no such correlation was observed with G3 formation, suggesting that multiple UGT isoforms, including UGT1A1 and UGT1A3, are involved in the G3 formation. G2 is also observed in rat and monkey liver microsomes as a major metabolite of T-5224, suggesting that G2 is not a human-specific metabolite. In this study, we obtained useful information on the metabolism of T-5224 for its clinical use.

## **Introduction**

T-5224, 3-{5-[4-(Cyclopentyloxy)-2-hydroxybenzoyl]-2-[(3-hydroxy-1, 2-benzisoxazol-6-yl) methoxy] phenyl} propionic acid, is a small molecule that was designed as an inhibitor of the c-Fos/activator protein-1 (AP-1) using three-dimensional, pharmacophore modeling (Tsuchida et al., 2004, 2006). Administration of T-5224 resolved type II collagen-induced arthritis in a preclinical model by reducing the amount of inflammatory cytokines and matrix metalloproteinases in sera and joints (Aikawa et al., 2008). Based on its pharmacological effects in arthritis, T-5224 has been developed as a therapeutic agent for rheumatoid arthritis. The phase I clinical trial was completed and the phase II clinical trial is in progress. For drug development, predicting the metabolism of a candidate compound in humans is important for estimating its safety to humans and any risks for drug-drug interactions. In animals, orally administered T-5224 is metabolized to form a glucuronide as its main metabolite (unpublished data). In phase I clinical study, the major metabolites in urine were glucuronides. Given that glucuronidation is the major clearance mechanism for T-5224 in human, it is important to predict its contribution to the human clearance of T-5224 and in evaluating drug-drug interactions.

Glucuronidation is catalyzed by UDP-glucuronosyltransferase (UGT) and is one of the most common phase II biotransformation reactions for therapeutic drugs. It was the clearance mechanism for approximately 1 in 10 drugs in the top 200 drugs prescribed in the United States in 2002 (Williams et al., 2004). Human UGTs are expressed in a tissue-specific manner in hepatic and extrahepatic tissues (Strassburg et al., 1998).

DMD #37952

However, unlike cytochrome P450s (P450s), the absolute content of UGTs in tissues has not been determined, and it is an important and difficult task to estimate the contributing ratio of individual UGT isoforms responsible for drug glucuronidation (Court, 2005 and 2010).

In this study, we used human liver microsomes (HLMs), human intestinal microsomes (HIMs) and recombinant human UGT isoforms expressed in baculovirus-infected insect cells to predict the metabolism of T-5224 in humans. We also successfully identified the chemical structures of two major T-5224 glucuronides and revealed the UGT isoforms responsible for its glucuronidation.

## **Materials and Methods**

**Materials.** T-5224 (Fig. 1) was synthesized at the Toyama Chemical Co., Ltd. (Tokyo, Japan). <sup>14</sup>C-labeled T-5224 was synthesized at the Daiichi Pure Chemicals Co., Ltd. (Ibaraki, Japan). UDP-glucuronic acid (UDPGA) was purchased from Nacalai Tesque Inc. (Kyoto, Japan). Alamethicin and  $\beta$ -estradiol were purchased from Sigma-Aldrich (St. Louis, MO). Two lots of pooled HLMs (4 males from 24–63 years old and 6 females from 34–52 years old; 8 males from 29–59 years old and 7 females from 21–58 years old) and HIMs (8 males from 16–71 years old and 7 females from 18–79 years old) from donors were purchased from Tissue Transformation Technologies (Edison, NJ). Microsomes from 7 individual human livers, including allelic variants, were purchased from BD Biosciences (Woburn, MA). The following lot numbers were purchased; HH629 (UGT1A1\*28\*28), HG43, HG18, HH650 (UGT1A1\*1\*1), HH855 (UGT1A1\*1\*28), HH741 and HH13. Recombinant human UGT (UGT1A1, UGT1A3, UGT1A4, UGT1A6, UGT1A7, UGT1A8, UGT1A9, UGT1A10, UGT2B4, UGT2B7, UGT2B15 and UGT2B17) and recombinant human P450 (CYP1A2, CYP2A6, CYP2B6, CYP2C8, CYP2C9\*1, CYP2C19, CYP2D6\*1, CYP2E1 and CYP3A4) were purchased from BD Biosciences. The UGT activity of  $\beta$ -estradiol (at the 3-OH position) in microsomes from 7 individual human livers was considered the typical UGT1A1 activity. The typical UGT activities and protein contents were used as described in the data sheets provided by the supplier. Antipeptide, anti-human UGT antibodies were previously produced in our laboratory (Kasai et al., 2004; Ikushiro et al., 2006). Endoglycosidase H (Endo H<sub>f</sub>) and N-glycosidase F (PNGase F) were purchased from New England Biolabs

Inc. (Ipswich, MA). All other chemicals and solvents were of analytical or the highest commercially available grade.

**Metabolism of T-5224 by recombinant human P450 isoforms.** The incubation mixture for the P450 reaction (500  $\mu$ L total volume) contained 100 mM Tris-HCl buffer (pH 7.5) or 100 mM potassium phosphate buffer (pH 7.4) (for CYP2A6 and CYP2C9\*1), 50 pmol/mL of each of the recombinant human P450s (CYP1A2, CYP2A6, CYP2B6, CYP2C8, CYP2C9\*1, CYP2C19, CYP2D6\*1, CYP2E1 and CYP3A4), a NADPH generating system, and 2  $\mu$ M of  $^{14}$ C-T-5224.  $^{14}$ C-T-5224 was dissolved in dimethyl sulfoxide (DMSO) with a final concentration of 0.5% (v/v) in the incubation mixtures. After incubation for 30 min at 37°C, the reaction was terminated by the addition of 1.5 mL of acetonitrile/methanol (1:1, v/v). The supernatant obtained by centrifugation (1800  $\times$  g for 10 min at 4°C) was subjected to high-performance liquid chromatography (HPLC) analysis using the CAPCELL PAK C<sub>18</sub>-MG analytical column (4.6  $\times$  150 mm, 3  $\mu$ m; Shiseido, Tokyo, Japan) at 40°C, and the radioactive peaks of the metabolites were detected. The mobile phase A was 5% (v/v) acetonitrile, the mobile phase B was 80% (v/v) acetonitrile, and both contained 30 mM of ammonium acetate. The following linear gradient was used: 0–100% B for 40 min, hold at 100% B for 20 min and hold at 0% B for 20 min. The flow rate was 1 mL/min.

**Glucuronidation of T-5224 in human liver microsomes, human intestinal microsomes and recombinant human UGT isoforms.** A typical incubation mixture (200  $\mu$ L total volume) contained the following: 50 mM Tris-HCl buffer (pH 7.5), 8 mM MgCl<sub>2</sub>, 0 to 50  $\mu$ M of

DMD #37952

T-5224, 0.1 or 0.01 mg/mL alamethicin, and 0.5 mg protein/mL pooled HLM, 0.25 mg protein/mL pooled HIM or 0.1 mg protein/mL recombinant human UGTs (UGT1A1, UGT1A3, UGT1A4, UGT1A6, UGT1A7, UGT1A8, UGT1A9, UGT1A10, UGT2B4, UGT2B7, UGT2B15 and UGT2B17). T-5224 was dissolved in DMSO at a final concentration of 2% (v/v) in the incubation mixtures. After preincubation at 37°C for 5 min, the reactions were initiated by adding UDPGA (2 mM). The reaction mixture was incubated at 37°C for 10 min (60 min for the recombinant human UGTs), and the reaction was terminated by the addition of acetonitrile (100  $\mu$ L). After removing the proteins by centrifugation at 13,000  $\times$  g for 20 min at 4°C, aliquots of the supernatants were injected into the HPLC. T-5224 and its glucuronides were monitored at 290 nm and eluted with the same conditions as described above except for the concentration of ammonium acetate in mobile phase (10 mM). Three T-5224 glucuronides, designated as G1, G2, and G3, were eluted. Due to the absence of authentic standards for T-5224 glucuronides, their amounts were estimated under the assumption that their absorption coefficients at 290 nm were the same as that of T-5224. In a separate study, purified G2 and G3 were both completely hydrolyzed with  $\beta$ -glucuronidase (type IX-A from *Escherichia coli*, Sigma-Aldrich) and detected as a single peak of T-5224 by HPLC.

**Enzymatic synthesis and extraction of the T-5224 glucuronides.** To synthesize the T-5224 glucuronides enzymatically, recombinant human UGT1A1 was expressed in yeast cells (Ikushiro et al., 2004). First, human UGT1A1 cDNA was isolated by reverse transcription-polymerase chain reaction (RT-PCR) from a total RNA

fraction prepared from human liver using the PCR primer set described as: (forward primer, cccaagcttaaaaaatggctgtggagtcccagggc; reverse primer, cccaagctttcaatgggtcttggatttgggctttctt).

To insert UGT1A1 cDNA into the pGYR expression vector, both primers contain *Hind* III sites. The resulting PCR fragment was digested with *Hind* III and inserted into the *Hind* III site of the vector pGYR, which contained a 2- $\mu$ m DNA ori, a *Leu2* gene as a marker, a *S. cerevisiae* NADPH-P450 reductase gene, pUC ori, *Amp<sup>r</sup>*, a glyceraldehydes-3-phosphate dehydrogenase (GAPDH) promoter and a terminator derived from *zygosaccharomyces rouxii*. The resulting plasmid pGYR-hUGT1A1 was introduced into *S. cerevisiae* AH22 cells as described previously (Oeda et al. 1985). The recombinant yeast cells expressing UGT1A1 were cultivated in a synthetic, minimal medium containing 2% (w/v) D-glucose and 0.67% (w/v) yeast nitrogen base without amino acids, supplemented with histidine (20 mg/L). The microsomal fractions were prepared as described previously (Oeda et al. 1985). The protein concentrations of the microsomes were determined with the bicinchoninic acid (BCA) protein assay reagent (Nacalai Tesque) using bovine serum albumin as a standard.

The reaction mixture (200 mL) contained 50 mM Tris-HCl buffer (pH 7.5), 8 mM MgCl<sub>2</sub>, 600 mg of yeast microsomes, 20  $\mu$ M T-5224 and 4 mM UDPGA. After incubation at 37°C for 24 hr, the reaction was terminated by the addition of acetonitrile (100 mL). After removal of the protein by centrifugation at 14,000  $\times$  g for 20 min at 4°C, the supernatant was evaporated under reduced pressure at room temperature to obtain the aqueous solvent containing the hydrophilic components. The aqueous solvent was transferred to solid-phase extraction cartridges (Oasis HLB, 60 mg/3 cc, Waters, Milford, MA), which were

DMD #37952

previously rinsed with 3 mL of methanol and water. Each cartridge was washed with water (3 mL) and eluted twice with methanol (3 mL), and finally, 120 mL of eluate was recovered. DMSO (200  $\mu$ L) was added to the eluate, which was concentrated to approximately 2 mL by evaporation under reduced pressure at room temperature. The resulting residue was injected onto a Develosil ODS-HG column (20  $\times$  250 mm, 5  $\mu$ m; Nomura Chemical, Aichi, Japan) at room temperature. The mobile phases A and B were the same as described above, and the following linear gradient was used: 0–100% B for 40 min and hold at 0% B for 10 min. The flow rate was 10 mL/min. Each fraction containing G2 (approximately 20 mL) or G3 (approximately 40 mL) was automatically collected with the fraction collector (FRC-10A, Shimadzu, Kyoto, Japan). DMSO (100  $\mu$ L) was added to each fraction, and the organic solvent was evaporated under reduced pressure at room temperature to obtain the aqueous solutions containing G2 or G3. The aqueous solutions were transferred to solid-phase extraction cartridges (Oasis MAX, 500 mg / 6 cc, Waters) that were previously rinsed with 3 mL of methanol and water. The cartridges were washed with 4 mL of water and methanol, and eluted twice with 5 mL of methanol containing 5% (v/v) formic acid. The eluates were evaporated to dryness under reduced pressure at room temperature to obtain G2 and G3, which were used for mass spectrometric analysis.

**Identification of T-5224 glucuronides by high-performance liquid chromatography/hybrid Fourier transform mass spectrometry.** The T-5224 glucuronides were analyzed by the HPLC/hybrid Fourier transform mass spectrometry (LC/hybrid FTMS) system (LTQ Orbitrap XL, Thermo Fisher Scientific, Waltham, MA). The HPLC conditions

were the same as described above except for the flow rate. The HPLC was operated in an isocratic mode with a flow rate of 0.5 mL/min, and the mobile phases A (50%) and B (50%) were mixed in an LC pump. The LTQ Orbitrap was operated in negative-ion mode and the settings were as follows: spray voltage 3.0 kV, resolution 30,000, and full MS mass range  $m/z$  150 – 1200. Glucuronides were analyzed in high-energy collision dissociation (HCD) mode with normalized collision energies of 30%, 40%, 50% and 60%.

**Alkaline hydrolysis of the T-5224 glucuronides.** The T-5224 glucuronides, G2 and G3, were each incubated with NaOH (0.17 M) for 2 hr at room temperature. The reactions were terminated by neutralization with HCl, and the products were analyzed by HPLC.

**Kinetic analyses.** Kinetic studies were performed using the pooled HLMS, pooled HIMs, and recombinant human UGTs (UGT1A1, UGT1A3 and UGT1A8). For determining the kinetic parameters, T-5224 concentrations (1 to 50  $\mu$ M) were used for analysis. The incubation times were 10 min except for the HIMs (20 min), which had lower T-5224 concentrations (below 5  $\mu$ M), and the recombinant human UGTs (60 min). Kinetic parameters were estimated from the fitted curves using the Kaleida Graph computer program (Synergy Software, Reading, PA), which was designed for nonlinear regression analysis. The following equations were applied for substrate inhibition kinetics (eq. 1):

$$V = \frac{V_{\max} \times S}{K_m + S + \frac{S^2}{K_{si}}} \quad (1)$$

where  $V$  is the rate of reaction,  $V_{\max}$  is the maximum velocity,  $K_m$  is the

DMD #37952

Michaelis constant,  $S$  is the substrate concentration, and  $K_{si}$  is the constant describing the substrate inhibition interaction (Houston and Kenworthy, 2000). A turnover number ( $k_{cat}$ ) was calculated as (eq. 2):

$$k_{cat} = \frac{V_{max}}{E_0} \quad (2)$$

where  $E_0$  is the UGT concentration. To estimate the *in vitro*, intrinsic clearance ( $CL_{int}$ ), the following equation was used (eq. 3):

$$CL_{int} = \frac{V_{max}}{K_m} \times \frac{\text{milligram of microsomal protein}}{\text{gram of tissue}} \times \frac{\text{gram of tissue}}{\text{killogram of body weight}} \quad (3)$$

As reported by Soars et al (2002), the  $CL_{int}$  values for T-5224 glucuronidation were calculated for the HLMs (45 mg microsomal protein/g liver and 20 g liver/kg body weight) and the HIMs (3 mg microsomal protein/g intestine and 30 g intestine/kg body weight).

**Effects of UDP-glucuronic acid concentrations on T-5224 glucuronidation.** To estimate the  $K_m$  value for UDPGA in T-5224 glucuronidation, a constant T-5224 concentration (10  $\mu$ M) was incubated with different UDPGA concentrations. The components of the incubation mixture were the same as described above. After preincubation at 37°C for 5 min, the reactions were initiated by adding UDPGA at final concentrations of 0, 0.1, 0.2, 0.4, 1, 2 or 4 mM. After incubation at 37°C for 10 min, the reactions were terminated by the addition of acetonitrile (100  $\mu$ L). The subsequent analyses were the same as described above. The following equation was applied for the Michaelis-Menten kinetics (eq. 4):

$$V = \frac{V_{max} \times S}{K_m + S} \quad (4)$$

**Inhibition analysis of T-5224 glucuronidation activity in human liver microsomes and recombinant human UGT1A1.**  $\beta$ -Estradiol (Senafi et al., 1994) is a typical substrate for UGT1A1. The inhibitory effects of  $\beta$ -estradiol on T-5224 glucuronidation were investigated with the pooled HLMs and recombinant human UGT1A1. The reaction mixtures contained T-5224 (10  $\mu$ M), UDPGA (2 mM),  $\beta$ -estradiol (0 to 500  $\mu$ M) and the same components as described above.  $\beta$ -estradiol was dissolved in DMSO; therefore, the reaction mixture contained 2% (v/v) of DMSO. After incubations at 37°C for 10 min (HLMs) or 60 min (UGT1A1), the reactions were terminated by the addition of acetonitrile (100  $\mu$ L). The subsequent analyses were the same as described above.

**Immunoblot analyses.** Polyclonal antibodies against each UGT isoform-specific peptide and a C-terminal peptide common to all human UGT1A or UGT2B isoforms have been developed in our laboratory (Kasai et al., 2004; Ikushiro et al., 2006) and were used for the detection of the UGTs. To obtain clear UGT bands on the immunoblots, microsomes were treated with Endo H<sub>f</sub> (recombinant UGT) or PNGase F (HLMs except for detecting UGT1A1) (New England Biolabs Inc., Ipswich, MA) according to the manufacturer's protocol and subjected to SDS-polyacrylamide gel electrophoresis as described previously (Ikushiro et al., 1995). The proteins in the gel were blotted to nitrocellulose membranes using a semi-dry blotting method. The membranes were blocked with 1.5% (w/v) bovine serum albumin or PVDF Blocking Reagent Can Get Signal<sup>®</sup> (TOYOBO) at room temperature. The membranes were incubated overnight with diluted primary antibodies (1:2000 to 1:32000 dilution with Can Get Signal<sup>®</sup> solution 1, TOYOBO) at room temperature. They were then incubated

with a diluted anti-primary antibody (1:2000 or 1:4000 dilution with Can Get Signal<sup>®</sup> solution 2, TOYOBO) of alkaline phosphatase-conjugated goat anti-rabbit IgG (Cell Signaling Technology Inc., Danvers, MA) at room temperature for 2 to 5 h. Immunodetection was developed by adding a nitro-blue tetrazolium chloride/5-bromo-4-chloro-3'-indolylphosphatase *p*-toluidine salt solution (1-Step<sup>™</sup> NBT/BCIP, Thermo Fisher Scientific, Waltham, MA). The band intensities were quantified using a densitometric scanner and NIH image software (ImageJ, Version 1.38). The UGT isoform contents expressed in recombinant UGT microsomes were quantified using anti-UGT1A or UGT2B antibodies. The recombinant UGT1A1 and UGT2B4 microsomes, with UGT contents known to be 1.6 and 0.6 nmol/mg protein, respectively, were used as standards (Kasai et al., 2004).

**Correlation Analyses.** The correlations between T-5224 and  $\beta$ -estradiol glucuronidation activity and between T-5224 glucuronidation activity and the expression levels of UGTs were determined in 7 individual HLMs. The Pearson's product-moment method was used to judge the correlations. A *p* value of less than 0.05 was considered statistically significant.

## **Results**

**T-5224 glucuronide formation in human liver and intestinal microsomes.** After incubating T-5224 with microsomes in the presence of UDPGA, two major peaks containing the glucuronides G2 and G3 were observed on HPLC chromatograms in the pooled HLMs and HIMs. A small peak containing glucuronide G1 were observed in the pooled HLMs (Fig. 2). Since the amounts of G1 formed were very low, we focused on G2 and G3 in the further studies. In pooled HLM and HIMs, both G2 and G3 increased linearly with increasing microsomal protein concentrations (0.1, 0.25, 0.5 and 1.0 mg/mL) or incubation times (5, 10, 20, and 30 min) (data not shown).

**Metabolism of T-5224 by recombinant human P450s and UGTs.** None of the P450 isoforms metabolized T-5224 (Supplemental Data Fig. s1), but multiple UGT isoforms showed significant T-5224 glucuronidation. Two major glucuronides, G2 and G3, were formed in the recombinant human UGTs with 5  $\mu$ M or 50  $\mu$ M of T-5224 (Fig. 3A and B). Quantitative immunoblot analyses were performed assuming that the reactivities of anti-UGT1A and UGT2B antibodies for each UGT subfamily were similar among each isoform. The protein content of each UGT in the microsomes were as follows: UGT1A1, UGT1A3, UGT1A4, UGT1A6, UGT1A7, UGT1A8, UGT1A9 and UGT1A10 were 2.6, 1.4, 2.3, 2.1, 1.7, 1.6, 1.7 and 3.1 nmol/mg protein, respectively and UGT2B4, UGT2B7, UGT2B15, UGT2B17 were 0.14, 0.75, 0.14 and 0.63 nmol/mg protein, respectively (Supplemental Data Fig. s2A). From these immunoblot analyses, T-5224 glucuronidation activities per UGT molecule ( $V/E_0$ ) were estimated for G2 and G3. G2 formation was only

catalyzed by UGT1A1 and UGT1A3. On the other hand, G3 formation was catalyzed by multiple UGT isoforms, and UGT1A1, UGT1A3, and UGT1A8 showed the highest activities among the other isoforms. Therefore, we focused on UGT1A1, UGT1A3, and UGT1A8 for the kinetic analyses. Two major glucuronide peaks (G2 and G3) and no G1 peak were observed on HPLC chromatograms in recombinant human UGT1A1, UGT1A3, and UGT1A8 (Fig. 3C). Both G2 and G3 formations increased linearly with increasing microsomal protein concentration (0.05, 0.1 and 0.2 mg/mL) or incubation time (10, 20, and 60 min) (data not shown).

**Mass spectrometric analysis of the T-5224 glucuronides.** The orbitrap electrospray mass spectra of the four peaks typically formed by the incubation of T-5224 with HLMs in the presence of UDPGA, had  $[M-H]^-$  ions at  $m/z$  868.23083 (G1,  $C_{41}H_4O_{20}N$ ),  $m/z$  692.19830 (G2,  $C_{35}H_{34}O_{14}N$ ),  $m/z$  692.19818 (G3,  $C_{35}H_{34}O_{14}N$ ) and  $m/z$  516.16595 (T-5224,  $C_{29}H_{26}O_8N$ ) with the mass accuracy between  $-0.85$  and  $0.30$  ppm (Fig. 4). These results suggest the possibility that G1 is a di-glucuronide of T-5224, while G2 and G3 are mono-glucuronides of T-5224. Purified G2 and G3 were analyzed in HCD mode. With varied normalized collision energies (30 – 60%), G2 and G3 showed precursor ions at  $m/z$  692 and product ions such as at  $m/z$  516 for the aglycon,  $m/z$  369 for the cleaved aglycon and  $m/z$  175 for the derivative of the glucuronic acid moiety (Fig. 5A and B). The product ion at  $m/z$  193 for the deprotonated glucuronic acid was only produced from G2, suggesting the possibility that G2 is an acyl *O*-glucuronide (Fig. 5A).

**Alkaline hydrolysis of the T-5224 glucuronides.** After incubating

the purified G2 and G3 with NaOH, 79% and 40% of G2 and G3, respectively, were hydrolyzed to form T-5224, suggesting that G2 is more unstable than G3. These results, together with the mass spectrometric analyses, strongly suggest that G2 is an acyl *O*-glucuronide and that G3 is either a hydroxyl *O*-glucuronide or *N*-glucuronide of T-5224.

**Kinetics of T-5224 glucuronidation in human liver and intestinal microsomes and recombinant human UGTs.** Kinetic analyses of T-5224 glucuronidation were performed in pooled HLMs, pooled HIMs and recombinant human UGTs (UGT1A1, UGT1A3 and UGT1A8). The data points were fitted to the substrate-inhibition equation (Fig. 6) to yield the kinetic parameters (Table 1 and 2). To calculate  $k_{cat}$  values, the UGT contents ( $E_0$ ) obtained from the immunoblot analyses were used: UGT1A1, UGT1A3 and UGT1A8 were 1.5, 1.0 and 1.9 nmol/mg protein, respectively (Supplemental data Fig. s2B). The pooled HIMs showed a comparable  $V_{max}/K_m$  value to the pooled HLMs for the G2 formation (HIM, 40.9  $\mu\text{L}/\text{min}/\text{mg}$  protein; HLM, 44.0  $\mu\text{L}/\text{min}/\text{mg}$  protein) and a higher  $V_{max}/K_m$  value than the pooled HLMs for the G3 formation (HIM, 34.6  $\mu\text{L}/\text{min}/\text{mg}$  protein; HLM, 19.5  $\mu\text{L}/\text{min}/\text{mg}$  protein). However, the pooled HIMs showed much lower  $CL_{int}$  values (G2, 3.68 mL/min/kg; G3, 3.12 mL/min/kg) than the pooled HLMs (G2, 39.6 mL/min/kg; G3, 17.5 mL/min/kg) (Table 1). In the pooled HLMs and recombinant human UGT1A1, the  $V_{max}/K_m$  and  $k_{cat}/K_m$  values for G2 (HLM, 44.0  $\mu\text{L}/\text{min}/\text{mg}$  protein; UGT1A1, 903  $\text{M}^{-1}\cdot\text{sec}^{-1}$ ) were higher than those for G3 (HLM, 19.5  $\mu\text{L}/\text{min}/\text{mg}$  protein; UGT1A1, 284  $\text{M}^{-1}\cdot\text{sec}^{-1}$ ). In contrast, in recombinant human UGT1A3, the  $k_{cat}/K_m$  value for G3 (774  $\text{M}^{-1}\cdot\text{sec}^{-1}$ ) was higher than that for G2 (252  $\text{M}^{-1}\cdot\text{sec}^{-1}$ ).

Recombinant human UGT1A3 showed a higher  $k_{cat}/K_m$  value than UGT1A1 for G3. Recombinant human UGT1A8 only catalyzed the formation of G3 with a  $k_{cat}/K_m$  value ( $303 \text{ M}^{-1}\cdot\text{sec}^{-1}$ ) similar to UGT1A1 (Table 2).

**Effects of UDP-glucuronic acid on T-5224 glucuronidation.** At varying concentrations of UDPGA, Michaelis-Menten kinetics were observed in the HLMs with  $10 \mu\text{M}$  of T-5224 (data not shown). The  $K_m$  values for UDPGA were different between G2 ( $1.8 \pm 0.2 \text{ mM}$ ) and G3 ( $0.74 \pm 0.04 \text{ mM}$ ), suggesting that the UGT isoforms responsible for G2 and G3 formation are different; however,  $V_{max}$  values for their formation were similar (G2,  $201 \pm 7.8 \text{ pmol/min/mg protein}$ ; G3,  $137 \pm 2.8 \text{ pmol/min/mg protein}$ ).

**Inhibition analyses of T-5224 glucuronidation activity in human liver microsomes and recombinant human UGT1A1.**  $\beta$ -estradiol, which is an UGT1A1-specific substrate, inhibited the G2 formation in both pooled HLMs and recombinant human UGT1A1 with  $\text{IC}_{50}$  values of  $39$  and  $24.9 \mu\text{M}$ , respectively. However,  $\beta$ -estradiol showed weak or no inhibition of G3 formation in pooled HLMs and recombinant human UGT1A1 (Fig. 7).

**Correlations of the glucuronidation activity between T-5224 and  $\beta$ -estradiol or UGT-isoform expression.** Among 7 individual HLMs, including homozygotes or heterozygotes of the UGT1A1\*28 allele, the interindividual difference in the formation activity of G2 (3.6-fold; coefficient of variation (CV) = 52%) was higher than that of G3 (2.1-fold; CV = 24%) (Fig. 8A). Also, the G2 formation activity was

DMD #37952

significantly correlated with the  $\beta$ -estradiol 3-glucuronidation (UGT1A1) activity ( $r = 0.939$ ,  $p < 0.005$ ), whereas the G3 formation activity was not significantly correlated to it ( $r = 0.568$ ) (Fig. 8B and C). Western blot analyses revealed interindividual variabilities in UGT expression among the 7 HLMs except for UGT1A6 and UGT1A9 (Fig. 9A). The levels of loading controls (calnexin and NADH-cytochrome  $b_5$  reductase) did not vary among individuals (data not shown). Therefore, correlations were analyzed between the glucuronidation activities and the expression level of UGT1A1 or UGT1A3. A high correlation was observed between UGT1A1 level and G2 formation activity ( $r = 0.985$ ,  $p < 0.00005$ ) (Fig. 9B) but not with G3 formation activity (Fig. 9C). High correlations were also not observed between expression levels and glucuronidation activity in UGT1A3 (data not shown). The liver microsomes from a homozygous UGT1A1\*28\*28 carrier (HH629) showed the lowest G2 and G3 formation activities among the 7 HLMs.

## **Discussion**

A February 2008 Food and Drug Administration (FDA) guidance strongly recommends human metabolic evaluations for new drugs. Additional safety assessments may also be needed for human-specific and putative-toxic metabolites, such as acylglucuronides. However, with phase II (conjugated) metabolites, which are generally more water soluble and pharmacologically inactive, the need for further evaluations can be eliminated. Thus, characterizing the metabolism of new drugs in humans is required.

Our animal studies revealed that the major T-5224 metabolites were glucuronides. Also glucuronide metabolites were major metabolites in human urine (data not shown). A comprehensive study is needed to clarify the clear elimination pathway of T-5224 including sulfonation and glucuronidation. To begin with, we focused glucuronidation and characterized T-5224 glucuronidation using HLMs, HIMs and recombinant human UGTs. We also estimated the contribution of each human UGT isoform to T-5224 glucuronidation, and verified if the glucuronide was an acylglucuronide.

As shown in Fig. 1, T-5224 is possibly conjugated at four positions: (1) carboxyl group, (2) OH group in a benzisoxazole, (3) NH group in a benzisoxazole, and (4) phenolic OH group. The mass spectrometric analyses of G2 and G3 using LC/hybrid FTMS showed different fragmentation patterns between G2 and G3 and different collision energies (30 – 60%). The fragment  $m/z$  193 was produced only from G2. Fenselau and Johnson (1980) and Niemeijer et al. (1991) reported that the O bond to the aromatic ring is not readily broken in the mass spectrometric analysis of phenols or phenol derivatives. The  $m/z$  193

ion is considered to be the deprotonated glucuronic acid ion produced by cleaving the carboxyl group C-O bond, as reported by Jaggi et al. (2002) and Plumb et al. (2007) on the acyl *O*-glucuronides of desmethylnaproxen and ibuprofen. Given the mass spectrometric analysis and that G2 is an alkali labile, this strongly suggests that G2 is the acyl *O*-glucuronide of T-5224. G2 was also observed as a major T-5224 metabolite in rat and monkey liver microsomes (Supplemental data Fig. s3), suggesting that G2 is not a human-specific metabolite. Therefore, animal studies could be important in the safety assessment of the T-5224 acyl *O*-glucuronide in humans. In addition, the amount of covalent binding of T-5224 and its metabolites (oxidation and conjugation products) in human liver S9 fractions and microsomes was much less than those of positive controls diclofenac and acetaminophen (data not shown). G3, another metabolite, showed no *m/z* 193 ion with any collision energy, indicating that G3 is the hydroxyl *O*-glucuronide or *N*-glucuronide of T-5224. A metabolite profiling study using nuclear magnetic resonance (NMR) and rat and monkey matrices showed the glucuronide that corresponds to G3 at the same retention time on the HPLC chromatogram was the hydroxyl *O*-glucuronide (the glucuronate conjugated position is “(2)”) (Supplemental data Fig. s4). In the <sup>1</sup>H-NMR spectrum of a glucuronide isolated from monkey bile, the proton signal of a hydroxyl group in a benzisoxazole was not detected, and the proton signals in a benzisoxazole were shifted. Furthermore, the proton signal of a phenolic hydroxyl group showed a similar chemical shift to that of T-5224. From these results, we propose the glucuronate-conjugated position of G3 as a hydroxyl group in a benzisoxazole.

The kinetic profiles for G2 and G3 exhibited the substrate inhibitions

for pooled HLMs, pooled HIMs, and recombinant human UGT1A1, UGT1A3 and UGT1A8. However, both  $K_m$  and  $K_{si}$  values for G2 ( $K_m = 4.93 \mu\text{M}$ ;  $K_{si} = 13.2 \mu\text{M}$ ) and G3 ( $K_m = 15.7 \mu\text{M}$ ;  $K_{si} = 27.0 \mu\text{M}$ ) were much higher in the pooled HLMs than an *in-vivo*  $ED_{50}$  for T-5224 corresponding to a  $C_{max}$  of 0.03 – 0.5  $\mu\text{M}$  (Aikawa et al., 2008). Based on these results, the equation (1) could be simplified to:

$$V = \frac{V_{max} \times S}{K_m} \quad (5)$$

Therefore, the physiologically, essential kinetic parameters are  $V_{max}/K_m$  and  $k_{cat}/K_m$  (Table 1 and 2).

UGT1A1, UGT1A3 and UGT1A8 appear to be essential for T-5224 metabolism (Fig. 3). Of these UGT isoforms, UGT1A8 is expressed in the human intestines but not in the human liver (Cheng et al., 1998; Fisher et al., 2001), and UGT1A1 and UGT1A3 are expressed in both the human liver and intestine (Strassburg et al., 1998; Fisher et al., 2001). The  $k_{cat}/K_m$  value of UGT1A8 for G3 was comparable to that of UGT1A1 (Table 2). This may indicate a large contribution of intestinal UGT1A8 to G3 formation. When drugs are administered orally, intestinal UGT and P450s have major roles in the first-pass metabolism (Fisher et al., 2001; Cubitt, 2009). However, the  $CL_{int}$  values estimated for G2 and G3 in the intestine were much lower than in the liver (Table 1), which suggests that the contribution of intestinal UGTs to T-5224 metabolism is negligible, and hepatic UGTs have important roles in this metabolism. Thus, we focused on UGT1A1 and UGT1A3 in the further analyses.

Recombinant human UGT1A1 showed a higher  $k_{cat}/K_m$  value for G2 ( $903 \text{ M}^{-1} \cdot \text{sec}^{-1}$ ) than for G3 ( $284 \text{ M}^{-1} \cdot \text{sec}^{-1}$ ). The UGT1A1  $k_{cat}/K_m$  value for G2 was significantly higher than that of UGT1A3 ( $252 \text{ M}^{-1} \cdot \text{sec}^{-1}$ ). A

typical UGT1A1 substrate  $\beta$ -estradiol significantly inhibited G2 formation (Fig.7). A high correlation was observed between G2 formation and  $\beta$ -estradiol 3-glucuronidation activities (Fig. 8B). These results strongly suggest that UGT1A1 is responsible for G2 formation. A high correlation between the UGT1A1 expression level and G2 formation activity confirmed this in the human liver (Fig. 9B).

Although recombinant UGT1A3 showed a much higher  $k_{cat}/K_m$  value than UGT1A1, no correlation was observed between G3 formation and the UGT1A3 expression level in the HLMs; however, a weak correlation was observed between G3 formation and the UGT1A1 expression level in the HLMs (Fig. 9C). In addition, a weak correlation was observed between G3 formation and  $\beta$ -estradiol 3-glucuronidation activity (Fig. 8C), which suggests a considerable contribution of UGT1A1 to the G3 formation in the human liver. Based on these results, the contribution of UGT1A1 appears to be larger than that of UGT1A3 for the G3 formation in the human liver. To our surprise,  $\beta$ -estradiol did not inhibit recombinant UGT1A1-dependent G3 formation, but it inhibited G2 formation (Fig. 7B). This may be due to an interaction between the T-5224 and  $\beta$ -estradiol in the UGT1A1 active site. UGT1A1-dependent glucuronidation of  $\beta$ -estradiol is reported to demonstrate homotropic activation kinetics in the presence of UGT1A1 substrates and other compounds (Williams et al., 2002). In another case, Zhou J et al. (2010) suggested that UGT1A4 has multiple aglycon binding sites and found that high-affinity UGT1A4 substrate tamoxifen activates and/or inhibits the formation of other UGT1A4 substrates (dihydrotestosterone and trans-androsterone). Based on these findings, it is possible to assume that  $\beta$ -estradiol could bind to substrate-binding pocket of UGT1A1 with T-5224 and inhibit the binding of T-5224 to catalyze the

formation of G2 but not G3.

To date, several reports have shown the relative expression of UGT mRNAs in the human liver (Congiu et al., 2002; Izukawa et al., 2009) and in multiple human tissues (Nishimura and Naito, 2006; Zhang et al., 2007; Nakamura et al., 2008; Ohno and Nakajin, 2009). In a more recent report from Court (2010), the relative abundance of UGT mRNAs in the human liver was summarized as the following: “highest” (UGT2B4); “high to medium” (UGT1A4, UGT2B7 and UGT2B15); “medium to low” (UGT1A1, UGT1A3, UGT1A6, UGT1A9 and UGT2B10); and “trace level or not detected” (UGT1A7 and UGT1A10). Incidentally, Ritter et al. (1999) found that the UGT1A1 mRNA levels were correlated with the UGT1A1 protein levels, and the UGT1A1 protein levels were correlated with human hepatic UGT1A1 activity. Based on these reports and our findings with recombinant UGT isoforms, UGT1A6, which was detected in all 7 individual HLMs, might have a small contribution to the G3 formation in the human liver (Fig. 3 and 9); however, UGT1A7 and UGT1A10 contributions appear to be negligible. The human UGT super-family comprises 19 isoforms. We have not evaluated the contribution of UGT1A5, UGT2B10, UGT2B11, UGT2B28, UGT2A1, UGT2A2 and UGT2A3 to T-5224 glucuronidation. The contribution of UGT1A5 and UGT2B28 to whole glucuronidation is likely to be small by the report (Court, 2010). UGT2B10 is reported to catalyze the *N*-glucuronidation with quaternary amines like tricyclic antidepressants (Zhou D et al., 2010). It is unlikely that UGT2B10 contributes to T-5224 metabolism because we could not confirm *N*-glucuronide of T-5224. The contribution of the other isozymes like UGT2A might be small, but cannot be neglected.

Including the homozygous UGT1A1\*28 allele, the interindividual

variability for the G2 formation, which is mainly catalyzed by UGT1A1, was higher (52% CV) than that for the G3 formation (24% CV), which is catalyzed by multiple UGT isoforms. These results indicate that the G2 formation may be a T-5224 metabolism-variation factor in humans. It should be noted that the magnitude of UGT-based drug interactions are generally smaller than the P450-mediated drug interactions (Lin & Wong, 2002; Willaims et al., 2004). The variabilities in the oral AUC of SN-38, the active metabolite of irinotecan, which is further conjugated by UGT1A1 and UGT1A9 (Iyer et al., 1998; Gagné et al., 2002), and its glucuronide were reported to be 3-fold in 9 patients with lung cancer, including those with the homozygous UGT1A1\*28 allele (Ando et al., 1998). More recently, Ramchandani et al. (2007) reported that the variability in the SN-38 AUC was approximately 10% (CV) in 82 patients including those homozygous for the UGT1A1\*28 allele. Considering that T-5224 has multiple glucuronidation pathways shared by multiple UGT isoforms, T-5224 most likely will not cause drug interaction via glucuronidation. However, we must monitor pharmacokinetic outcomes of T-5224 when it is co-administrated with typical UGT inhibitors or inducers (Kiang et al., 2005).

In conclusion, our study found the following: (1) T-5224 is metabolized to form two major, isomeric glucuronides, and one of them is an acyl *O*-glucuronide which was also detected in rats and monkeys as a major metabolite; (2) UGT1A1 and UGT1A3 have central roles in the glucuronidation of T-5224, and UGT1A1 is responsible for the formation of the acyl *O*-glucuronide; and (3) Interindividual differences in the glucuronidation of T-5224 were not very large, even with a homozygous UGT1A1\*28 allele. Therefore, *in-vitro* T-5224 metabolism studies provide useful information to study the safety of

DMD #37952

T-5224 in humans.

### **Acknowledgements**

The authors thank Dr. Kozo Hori, Dr. Yukihiro Aikawa, Mr. Masaki Shimizu, Mr. Yoshitaka Yamamoto and Mr. Masaki Katai from the Research Laboratories at Toyama Chemical Co., Ltd. for their useful advice and experimental support. The authors are grateful to the ADME/TOX Research Institute at Daiichi Pure Chemicals for the synthesis of  $^{14}\text{C}$ -T-5224 and the metabolite profiling.

**Authorship Contributions**

**Participated in research design:**

Uchihashi, Onoda, Hayakawa, Ikushiro and Sakaki.

**Conducted experiments:**

Uchihashi and Fukumoto.

**Contributed new reagents or analytic tools:**

Ikushiro.

**Performed data analysis:**

Uchihashi and Fukumoto.

**Wrote or contributed to the writing of the manuscript:**

Uchihashi, Onoda, Hayakawa, Ikushiro and Sakaki.

## **References**

- Aikawa Y, Morimoto K, Yamamoto T, Chaki H, Hashiramoto A, Narita H, Hirono S and Shiozawa S. (2008) Treatment of arthritis with a selective inhibitor of c-Fos/activator protein-1. *Nat Biotechnol* **26**: 817-823.
- Ando Y, Saka H, Asai G, Sugiura S, Shimokata K and Kamataki T (1998) UGT1A1 genotypes and glucuronidation of SN-38, the active metabolite of irinotecan. *Ann Oncol* **9**: 845-847.
- Cheng Z, Radominska-Pandya A and Tephly TR (1998) Cloning and expression of human UDP-glucuronosyltransferase (UGT) 1A8. *Arch Biochem Biophys* **356**: 301-305.
- Congiu M, Mashford ML, Slavin JL and Desmond PV (2002) UDP glucuronosyltransferase mRNA levels in human liver disease. *Drug Metab Dispos* **30**: 129-134.
- Court MH (2005) Isoform-selective probe substrates for *in vitro* studies of human UDP-glucuronosyltransferases. *Methods Enzymol* **400**: 104-116.
- Court MH (2010) Interindividual variability in hepatic drug glucuronidation: studies into the role of age, sex, enzyme inducers, and genetic polymorphism using the human liver bank as a model system. *Drug Metab Rev* **42**: 202-217.
- Cubitt HE, Houston JB and Galetin A (2009) Relative importance of intestinal and hepatic glucuronidation-impact on the prediction of drug clearance. *Pharm Res* **26**: 1073-1083.
- Fenselau C, Johnson LP (1980) Analysis of intact glucuronides by mass spectrometry and gas chromatography-mass spectrometry. A review. *Drug Metab Dispos* **8**: 274-83.

- Fisher MB, Paine MF, Strelevitz TJ and Wrighton SA (2001) The role of hepatic and extrahepatic UDP-glucuronosyltransferases in human drug metabolism. *Drug Metab Rev* **33**: 273-297.
- Gagné JF, Montminy V, Belanger P, Journault K, Gaucher G and Guillemette C (2002) Common human UGT1A polymorphisms and the altered metabolism of irinotecan active metabolite 7-ethyl-10-hydroxycamptothecin (SN-38). *Mol Pharmacol* **62**: 608-617.
- Houston JB and Kenworthy KE (2000) In vitro-in vivo scaling of CYP kinetic data not consistent with the classical Michaelis-Menten model. *Drug Metab Dispos* **28**: 246-254.
- Ikushiro S, Emi Y and Iyanagi T (1995) Identification and analysis of drug-responsive expression of UDP-glucuronosyltransferase family 1 (UGT1) isozyme in rat hepatic microsomes using anti-peptide antibodies. *Arch Biochem Biophys* **324**: 267-272.
- Ikushiro S, Sahara M, Emi Y, Yabusaki Y and Iyanagi T (2004) Functional coexpression of xenobiotic metabolizing enzymes, rat cytochrome P450 1A1 and UDP-glucuronosyltransferase 1A6, in yeast microsomes. *Biochimica Biophysica Acta* **1672**: 86-92.
- Ikushiro S, Emi Y, Kato Y, Yamada S and Sakaki T (2006) Monospecific antipeptide antibodies against human hepatic UDP-glucuronosyltransferase 1A subfamily (UGT1A) isoforms. *Drug Metab Pharmacokinet* **21**: 70-74.
- Iyer L, King CD, Whittington PF, Green MD, Roy SK, Tephly TR, Coffman BL and Ratain MJ (1998) Genetic predisposition to the metabolism of irinotecan (CPT-11). Role of uridine diphosphate glucuronosyltransferase isoform 1A1 in the glucuronidation of its active metabolite (SN-38) in human liver microsomes. *J Clin*

*Invest* **15**: 847-854.

Izukawa T, Nakajima M, Fujiwara R, Yamanaka H, Fukami T, Takamiya M, Aoki Y, Ikushiro S, Sakaki T and Yokoi T (2009) Quantitative analysis of UDP-glucuronosyltransferase (UGT) 1A and UGT2B expression levels in human livers. *Drug Metab Dispos* **37**: 1759-1768.

Jaggi R, Addison RS, King AR, Suthers BD and Dickinson RG (2002) Conjugation of desmethylnaproxen in the rat—a novel acyl glucuronide-sulfate diconjugate as a major biliary metabolite. *Drug Metab Dispos* **30**: 161-166.

Kasai N, Sakaki T, Shinkyo R, Ikushiro S, Iyanagi T, Kamao M, Okano T, Ohta M, Inouye K (2004) Sequential metabolism of 2,3,7-trichlorodibenzo-*p*-dioxin (2,3,7-triCDD) by cytochrome P450 and UDP-glucuronosyltransferase in human liver microsomes. *Drug Metab Dispos* **32**: 870-875.

Kiang TK, Ensom MH and Chang TK (2005) UDP-glucuronosyltransferases and clinical drug-drug interactions. *Pharmacol Ther* **106**: 97-132.

Lin JH and Wong BK (2002) Complexities of glucuronidation affecting in vitro-in vivo extrapolation. *Curr Drug Metab* **3**: 623-646.

Nakamura A, Nakajima M, Yamanaka H, Fujiwara R and Yokoi T (2008) Expression of UGT1A and UGT2B mRNA in human normal tissues and various cell lines. *Drug Metab Dispos* **36**: 1461-1464.

Niemeijer NR, Gerding TK, De Zeeuw RA (1991) Glucuronidation of labetalol at the two hydroxy positions by bovine livermicrosomes. Isolation, purification, and structure

elucidation of the glucuronides of labetalol. *Drug Metab Dispos* **19**: 20-3.

Nishimura M and Naito S (2006) Tissue-specific mRNA expression profiles of human phase I metabolizing enzymes except for cytochrome P450 and phase II metabolizing enzymes. *Drug Metab Pharmacokinet* **21**: 357-374.

Oeda K, Sakaki T and Ohkawa H (1985) Expression of rat liver cytochrome P-450MC cDNA in *Saccharomyces cerevisiae*. *DNA* **4**: 203-210.

Ohno S and Nakajin S (2009) Determination of mRNA expression of human UDP-glucuronosyltransferases and application for localization in various human tissues by real-time reverse transcriptase-polymerase chain reaction. *Drug Metab Dispos* **37**: 32-40.

Plumb RS, Rainville PD, Potts WB 3rd, Castro-Perez JM, Johnson KA and Wilson ID (2007) High-temperature ultra-performance liquid chromatography coupled to hybrid quadrupole time-of-flight mass spectrometry applied to ibuprofen metabolites in human urine. *Rapid Commun Mass Spectrom* **21**: 4079-4085.

Ramchandani RP, Wang Y, Booth BP, Ibrahim A, Johnson JR, Rahman A, Mehta M, Innocenti F, Ratain MJ and Gobburu JV (2007) The role of SN-38 exposure, UGT1A1\*28 polymorphism, and baseline bilirubin level in predicting severe irinotecan toxicity. *J Clin Pharmacol* **47**: 78-86.

Ritter JK, Kessler FK, Thompson MT, Grove AD, Auyeung DJ and Fisher RA (1999) Expression and inducibility of the human bilirubin UDP-glucuronosyltransferase UGT1A1 in liver and

cultured primary hepatocytes: evidence for both genetic and environmental influences. *Hepatology* **30**: 476-484.

Senafi SB, Clarke DJ and Burchell B (1994) Investigation of the substrate specificity of a cloned expressed human bilirubin UDP-glucuronosyltransferase: UDP-sugar specificity and involvement in steroid and xenobiotic glucuronidation. *Biochem J* **303**: 233-240.

Soars MG, Burchell B and Riley RJ (2002) In vitro analysis of human drug glucuronidation and prediction of in vivo metabolic clearance. *J Pharmacol Exp Ther* **30**: 382-390.

Strassburg CP, Manns MP and Tukey RH (1998) Expression of the UDP-glucuronosyltransferase 1A locus in human colon. Identification and characterization of the novel extrahepatic UGT1A8. *J Biol Chem* **273**: 8719-8726.

Tsuchida K, Chaki H, Takakura T, Yokotani J, Aikawa Y, Shiozawa S, Gouda H, Hirono S (2004) Design, synthesis, and biological evaluation of new cyclic disulfide decapeptides that inhibit the binding of AP-1 to DNA. *J Med Chem* **47**: 4239-4246.

Tsuchida K, Chaki H, Takakura T, Kotsubo H, Tanaka T, Aikawa Y, Shiozawa S, Hirono S (2006) Discovery of nonpeptidic small-molecule AP-1 inhibitors: lead hopping based on a three-dimensional pharmacophore model. *J Med Chem* **49**: 80-91.

Williams JA, Ring BJ, Cantrell VE, Campanale K, Jones DR, Hall SD and Wrighton SA (2002) Differential modulation of UDP-glucuronosyltransferase 1A1 (UGT1A1)-catalyzed estradiol-3-glucuronidation by the addition of UGT1A1 substrates and other compounds to human liver microsomes.

*Drug Metab Dispos* **30**: 1266-1273.

Williams JA, Hyland R, Jones BC, Smith DA, Hurst S, Goosen TC, Peterkin V, Koup JR and Ball SE (2004) Drug-drug interactions for UDP-glucuronosyltransferase substrates: a pharmacokinetic explanation for typically observed low exposure (AUC<sub>i</sub>/AUC) ratios. *Drug Metab Dispos* **32**: 1201-1208.

Zhang W, Liu W, Innocenti F and Ratain MJ (2007) Searching for tissue-specific expression pattern-linked nucleotides of UGT1A isoforms. *PLoS ONE* **2**: e396.

Zhou J, Tracy TS, Rimmel RP (2010) Glucuronidation of dihydrotestosterone and trans-androsterone by recombinant UDP-glucuronosyltransferase (UGT) 1A4: evidence for multiple UGT1A4 aglycone binding sites. *Drug Metab Dispos* **38**: 431-440.

Zhou D, Guo J, Linnenbach AJ, Booth-Genthe CL, Grimm SW (2010) Role of human UGT2B10 in N-glucuronidation of tricyclic antidepressants, amitriptyline, imipramine, clomipramine, and trimipramine. *Drug Metab Dispos* **38**: 863-870.

## **Figure Legends**

### **Fig. 1**

Chemical structure of T-5224 and proposed chemical structure of T-5224 glucuronide.

### **Fig. 2**

HPLC profiles of T-5224 and its glucuronides. T-5224 (10  $\mu\text{M}$ ) was incubated at 37°C with UDP-glucuronic acid for 10 min in pooled human liver microsomes (A) and intestinal microsomes (B).

### **Fig. 3**

T-5224 glucuronidation activity in each recombinant human UGT isoform. T-5224 was incubated at 5  $\mu\text{M}$  (A) or 50  $\mu\text{M}$  (B) for 60 min at 37°C with UDP-glucuronic acid, and the HPLC profiles of the recombinant human UGT1A1, UGT1A3 and UGT1A8 are shown (C). The incubations were performed in duplicate, and the glucuronidation activities ( $V/E_0$ ) were calculated with the UGT content obtained by immunoblot analyses. Glucuronides were not detected in UGT1A4, UGT1A9, UGT2B4, UGT2B7, UGT2B15, UGT2B17 and Mock.

### **Fig. 4**

Orbitrap electrospray mass spectra of the LC peaks for T-5224 glucuronides G1 (A), G2 (B), G3 (C) and T-5224 (D) in the negative-ion mode.

### **Fig. 5**

Product-ion mass spectra of T-5224 glucuronides G2 (A) and G3 (B)

analyzed by the high energy collision dissociation (HCD) mode, normalized collision energies between 30% and 60%, and their proposed chemical structures and mass fragmentations.

**Fig. 6**

Kinetics of T-5224 glucuronidation in pooled human liver microsomes (A), pooled human intestinal microsomes (B), and recombinant human UGT1A1 (C), UGT1A3 (D) and UGT1A8 (E). Each value ( $n = 3$ ) and fitting curve are plotted. T-5224 (1 – 50  $\mu\text{M}$ ) was incubated for 10 min (human liver and intestinal microsomes; 10 – 50  $\mu\text{M}$  of T-5224), 20 min (human intestinal microsomes; 1 – 5  $\mu\text{M}$  of T-5224) or 60 min (recombinant human UGT; 10 – 50  $\mu\text{M}$  of T-5224) at 37°C.

**Fig. 7**

Inhibitory effect of  $\beta$ -estradiol on G2 and G3 formation in pooled human liver microsomes (A) and recombinant human UGT1A1 (B). T-5224 (10  $\mu\text{M}$ ) was incubated for 10 min at 37°C in the absence or presence of  $\beta$ -estradiol (0 – 500 $\mu\text{M}$ ). Each value represents the mean  $\pm$  standard deviation ( $n = 3$ ).

**Fig. 8**

Interindividual variabilities in T-5224 glucuronidation activities in microsomes from 7 human livers (A). Lot HH629 is a homozygous carrier and lot HH855 is a heterozygous carrier of the UGT1A1\*28 allele. T-5224 (10  $\mu\text{M}$ ) was incubated in individual human liver microsomes for 10 min at 37°C. Each column represents the mean  $\pm$  standard deviation ( $n = 3$ ). Correlations between T-5224

DMD #37952

glucuronidation activities (G2 and G3) and  $\beta$ -estradiol 3-glucuronidation activity in microsomes from 7 human livers (B and C).

**Fig. 9**

Interindividual variabilities in the expression levels of human UGT isoforms in microsomes from 7 human livers (A). Microsomes containing 10 or 20  $\mu$ g protein were used in the immunoblot analyses. Lot HH629 is a homozygous carrier and lot HH855 is a heterozygous carrier of the UGT1A1\*28 allele. Correlations between the relative expression levels of UGT1A1 and G2 formation activity (B) or G3 formation activity (C). Quantitative immunodetection was performed for UGT1A1 and UGT1A3 in triplicate.

**Table 1**

Kinetic parameters of T-5224 glucuronidation in pooled HLM and pooled HIM.

Each value represents a best-fit value  $\pm$  computer-calculated standard error of triplicate points.

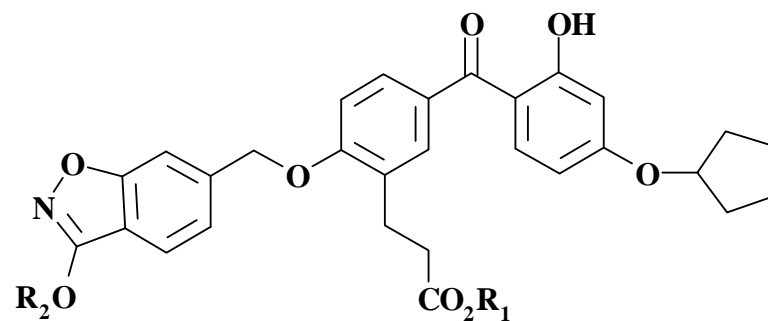
Protein source	G2					G3				
	$V_{\max}$	$K_m$	$K_{si}$	$V_{\max} / K_m$	$CL_{int}$	$V_{\max}$	$K_m$	$K_{si}$	$V_{\max} / K_m$	$CL_{int}$
	<i>pmol/min/mg protein</i>	$\mu M$	$\mu M$	$\mu L/min/mgprotein$	<i>mL/min/kg</i>	<i>pmol/min/mg protein</i>	$\mu M$	$\mu M$	$\mu L/min/mgprotein$	<i>mL/min/kg</i>
HLM	217 $\pm$ 33	4.93 $\pm$ 1.22	13.2 $\pm$ 3.2	44.0	39.6	305 $\pm$ 47	15.7 $\pm$ 3.4	27.0 $\pm$ 6.9	19.5	17.5
HIM	241 $\pm$ 118	5.88 $\pm$ 3.69	2.64 $\pm$ 1.62	40.9	3.68	106 $\pm$ 18	3.06 $\pm$ 1.12	58.0 $\pm$ 27.1	34.6	3.12

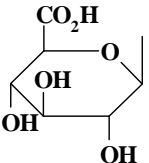
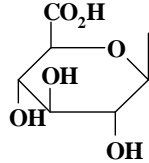
**Table 2**

Kinetic parameters of T-5224 glucuronidation for G2 and G3 in recombinant human UGT isoforms. Each value represents a best-fit value  $\pm$  computer-calculated standard error of triplicate points.

Glucuronide	UGT isoform	$V_{\max}$	$K_m$	$K_{si}$	$V_{\max} / K_m$	$k_{\text{cat}}$	$k_{\text{cat}} / K_m$
		<i>pmol/min/mg protein</i>	$\mu M$	$\mu M$	$\mu L/min/mg protein$	<i>sec<sup>-1</sup></i>	<i>M<sup>-1</sup>·sec<sup>-1</sup></i>
G2	1A1	664 $\pm$ 410	7.91 $\pm$ 5.89	1.54 $\pm$ 1.11	83.9	7.20 $\times 10^{-3}$	903
	1A3	112 $\pm$ 27	7.21 $\pm$ 2.64	13.5 $\pm$ 5.0	15.5	1.82 $\times 10^{-3}$	252
G3	1A1	146 $\pm$ 73	5.56 $\pm$ 3.85	4.67 $\pm$ 3.12	26.2	1.58 $\times 10^{-3}$	284
	1A3	849 $\pm$ 485	17.9 $\pm$ 11.8	2.55 $\pm$ 1.67	47.5	1.38 $\times 10^{-2}$	774
	1A8	206 $\pm$ 88	6.05 $\pm$ 3.44	3.64 $\pm$ 2.00	34.0	1.84 $\times 10^{-3}$	303

# Fig. 1



	$R_1$	$R_2$
<b>T-5224</b>	<b>H</b>	<b>H</b>
<b>T-5224 G2</b> (Acyl <i>O</i> -glucuronide)		<b>H</b>
<b>T-5224 G3</b> (Hydroxyl <i>O</i> -glucuronide)	<b>H</b>	

# Fig. 2

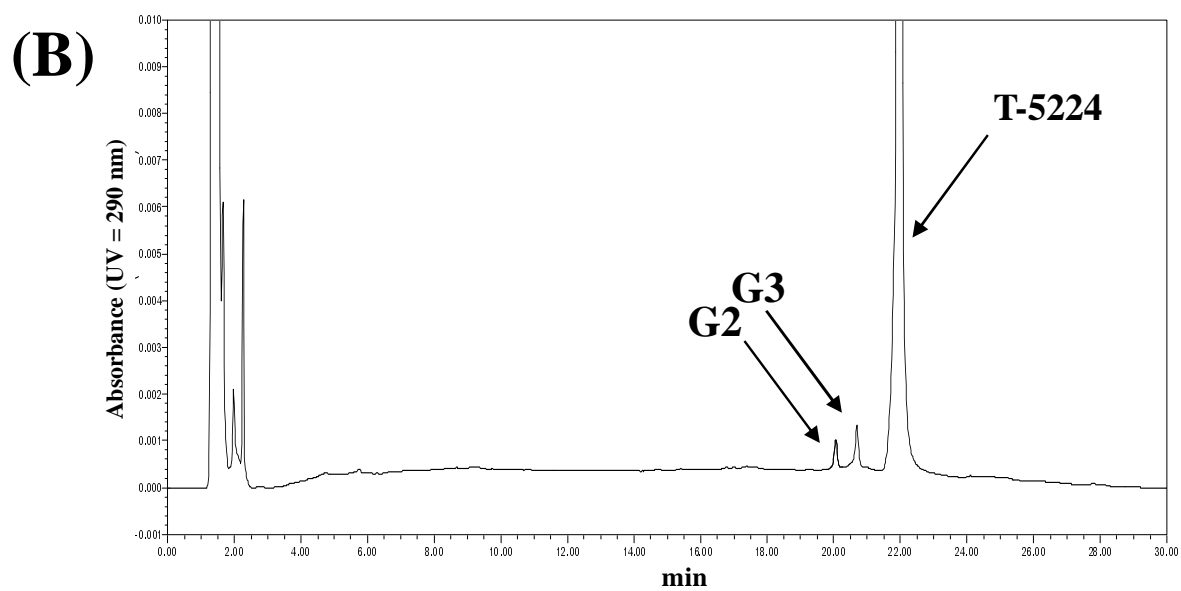
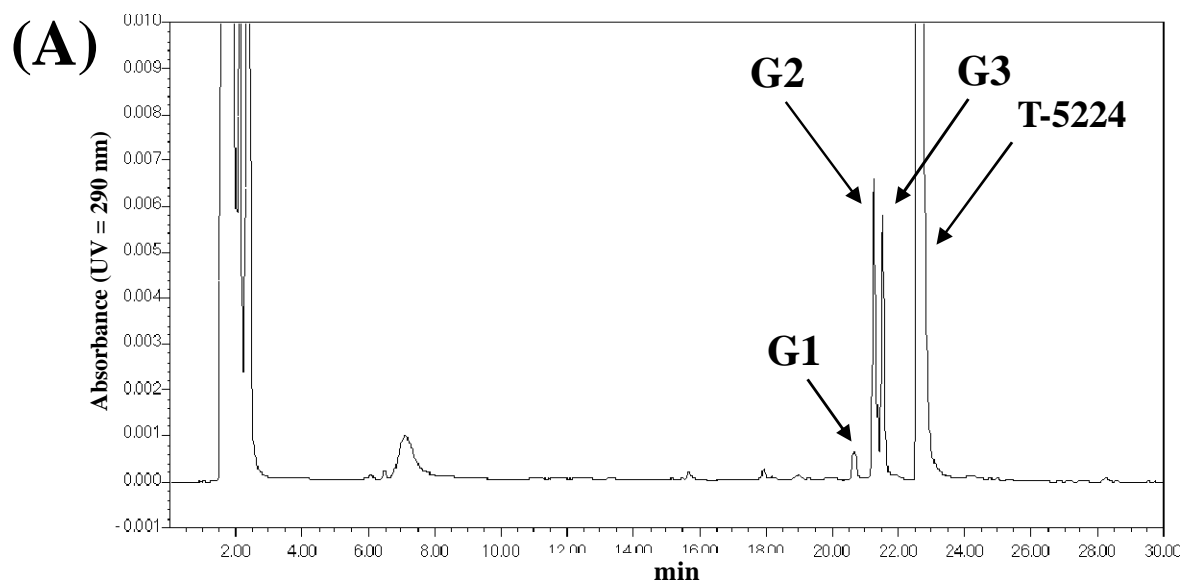


# Fig. 3

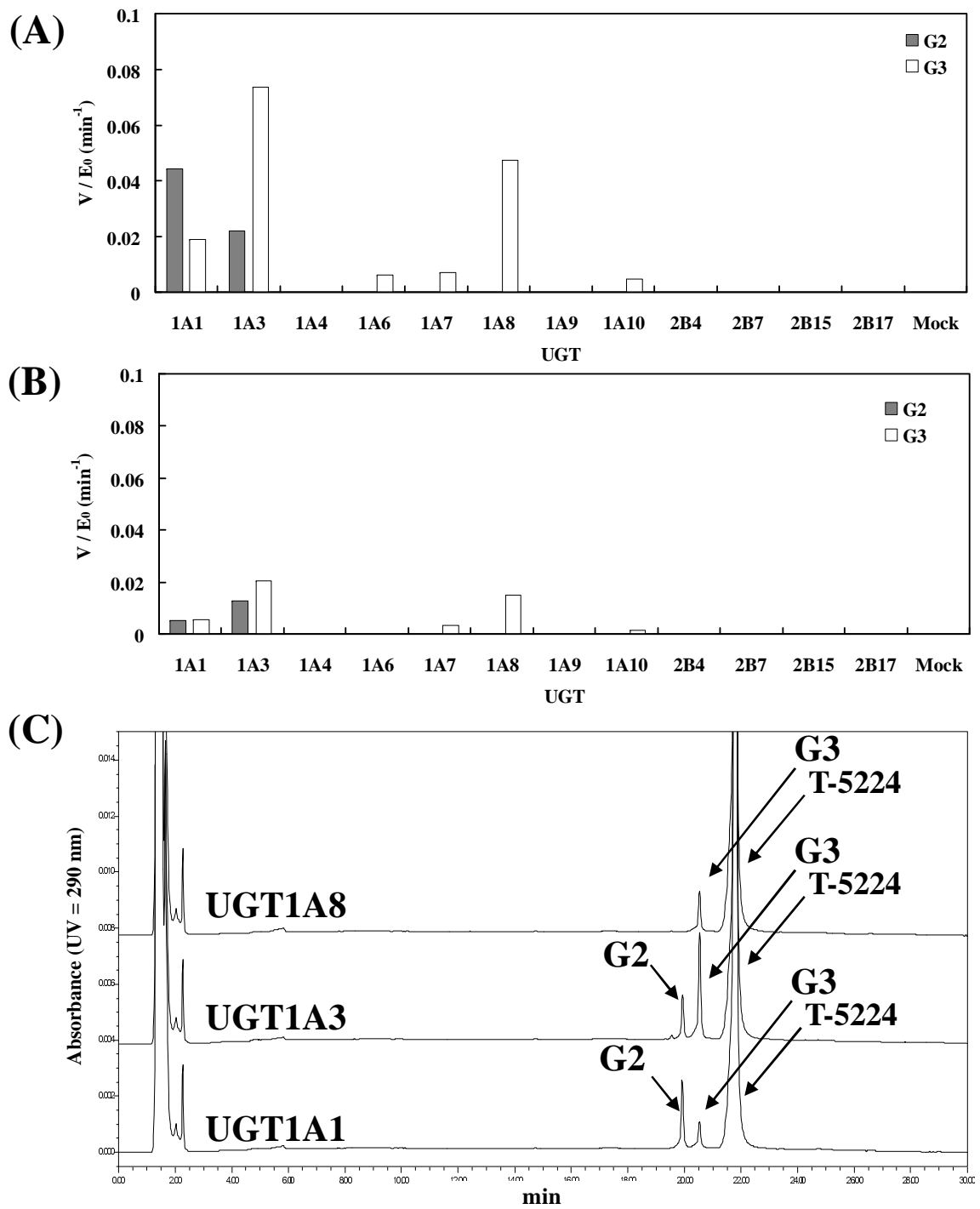


# Fig. 4

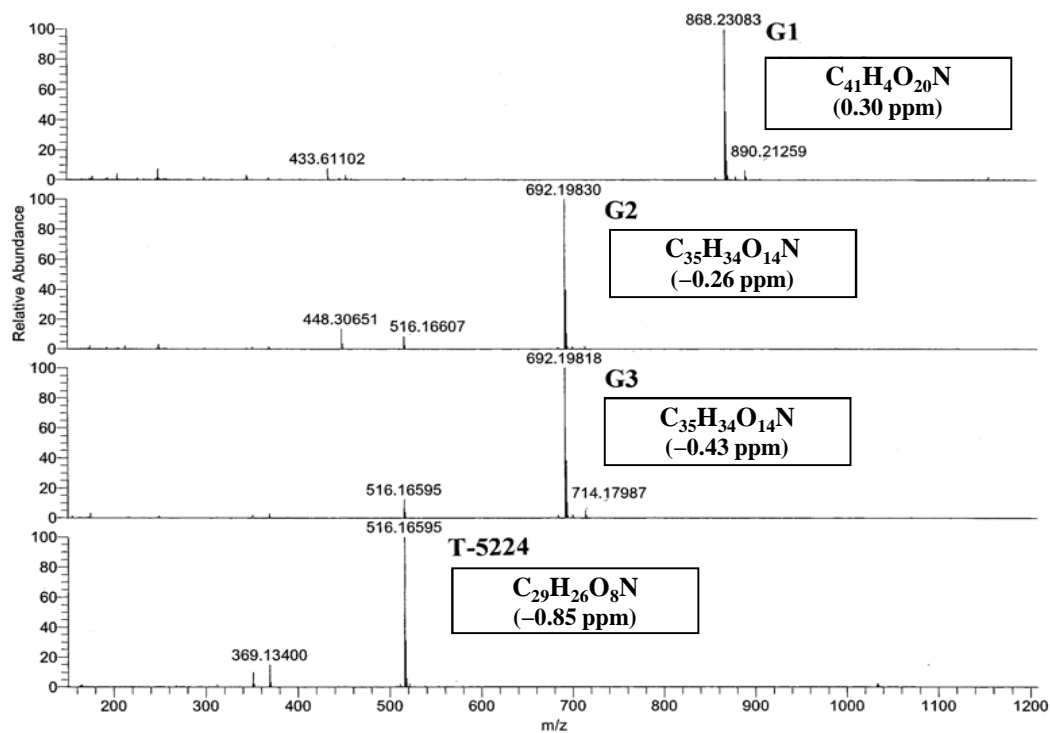
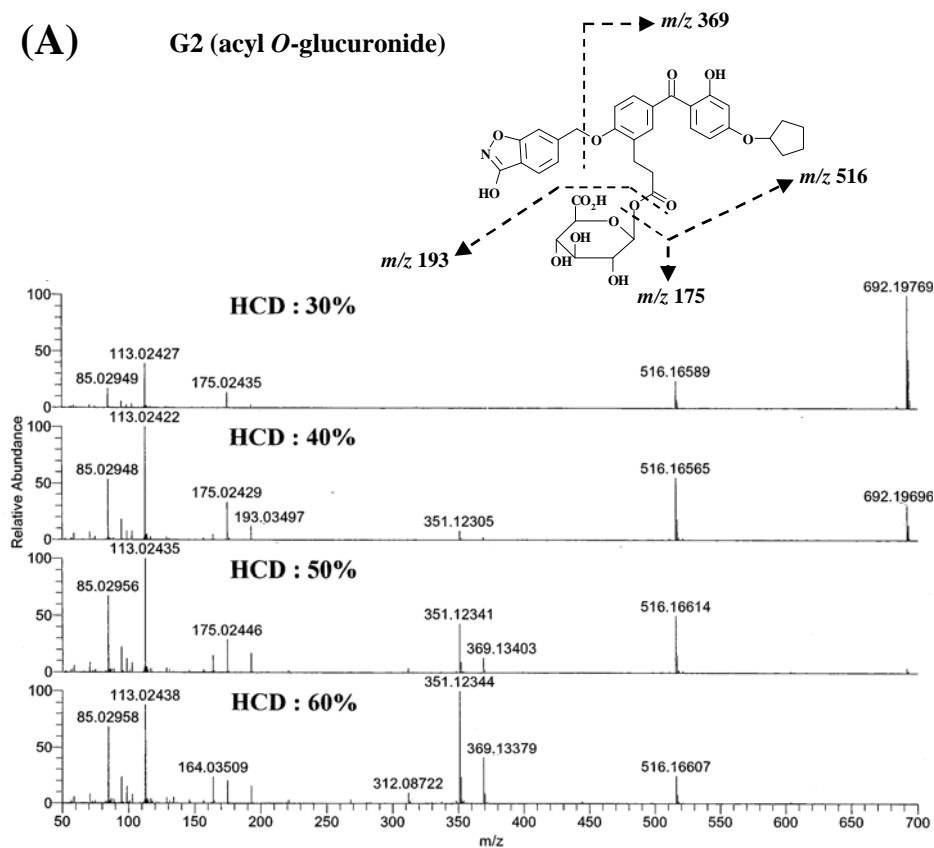


# Fig. 5

(A) G2 (acyl *O*-glucuronide)



(B) G3 (hydroxyl *O*-glucuronide)

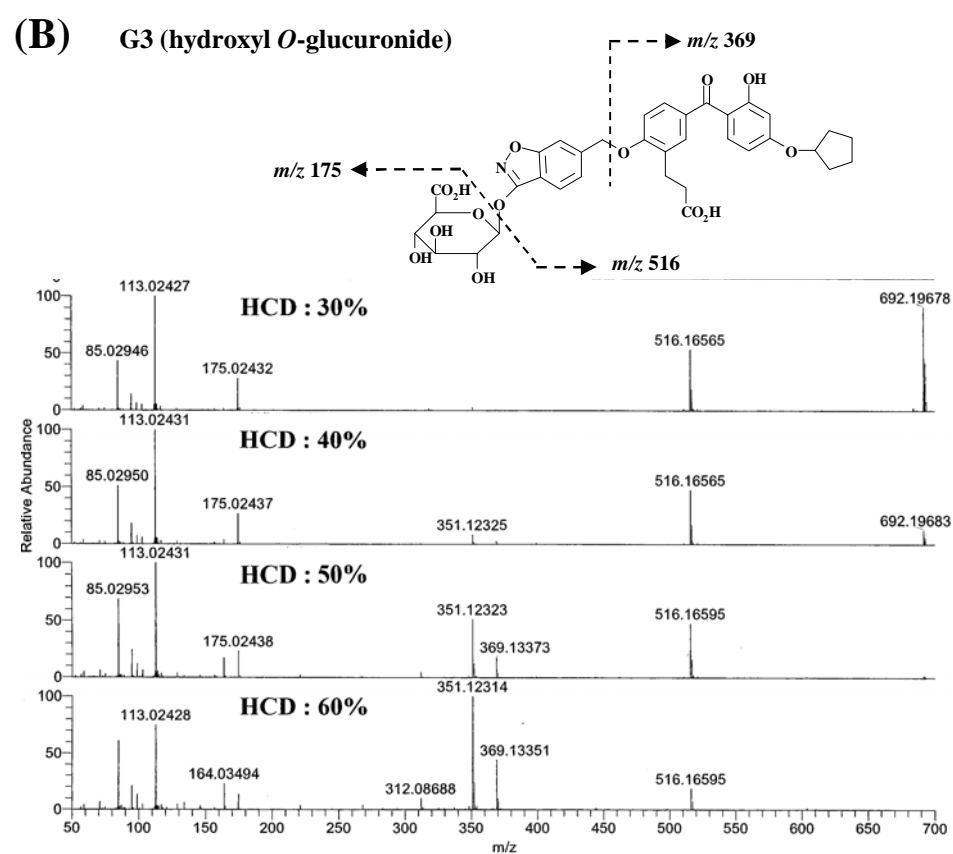


# Fig. 6

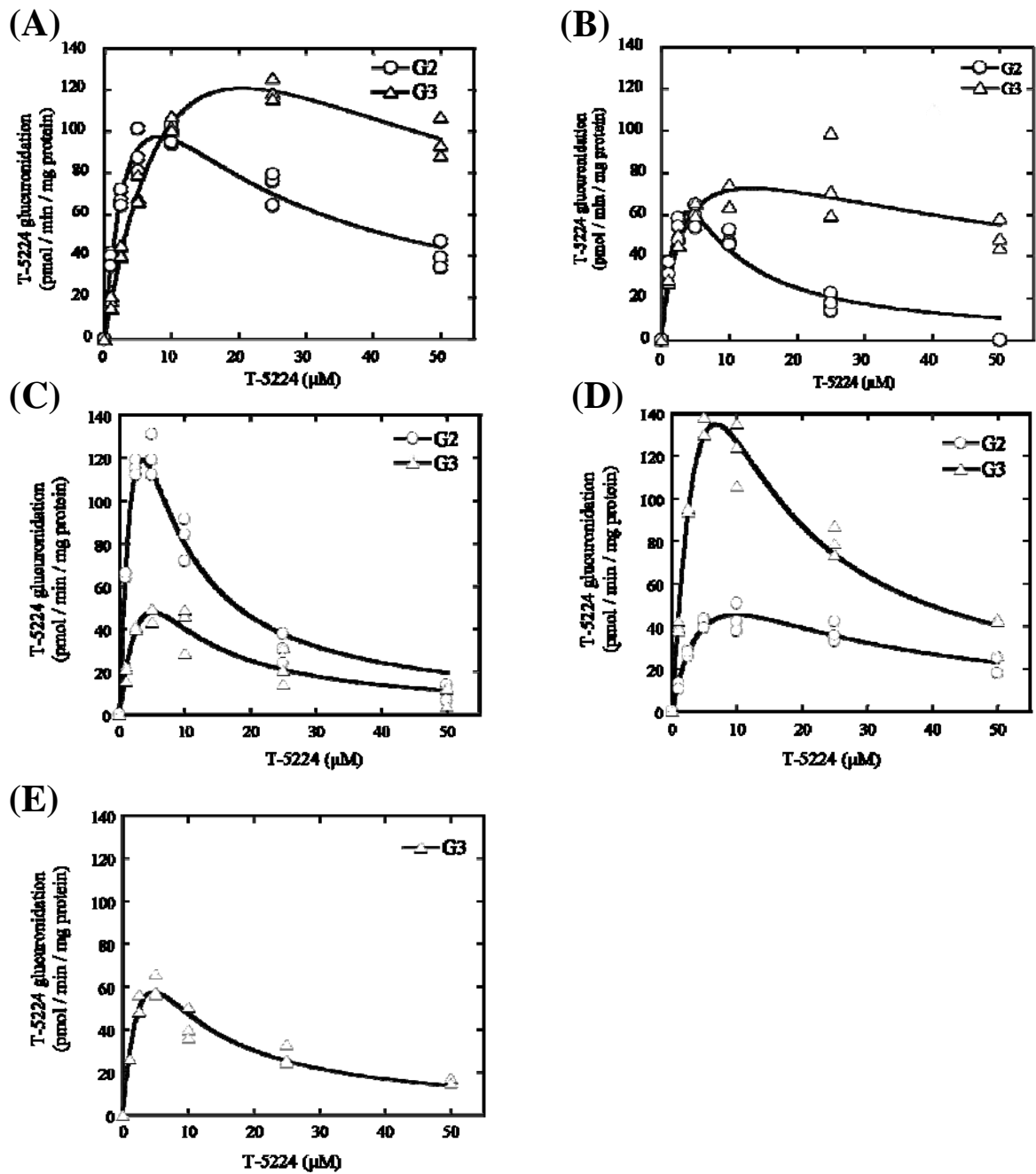


# Fig. 7

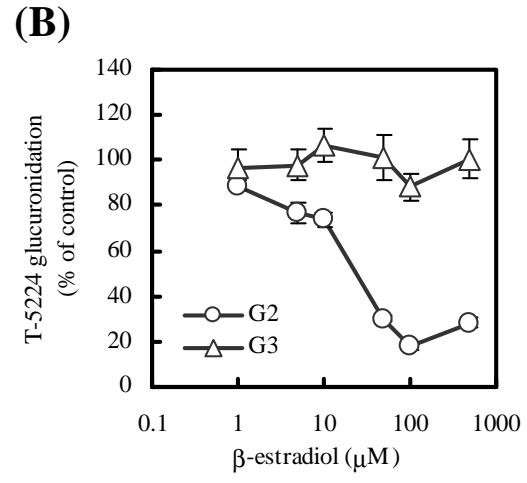
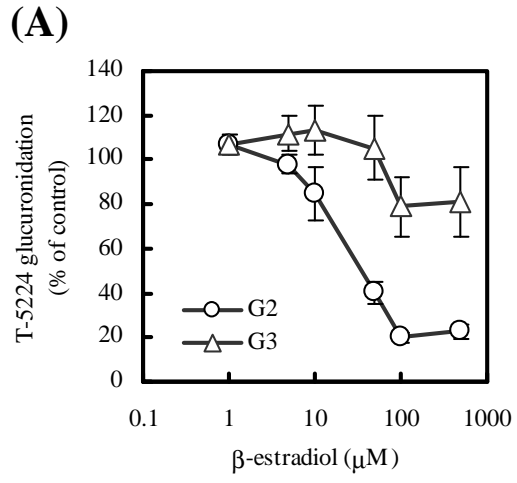


# Fig. 8

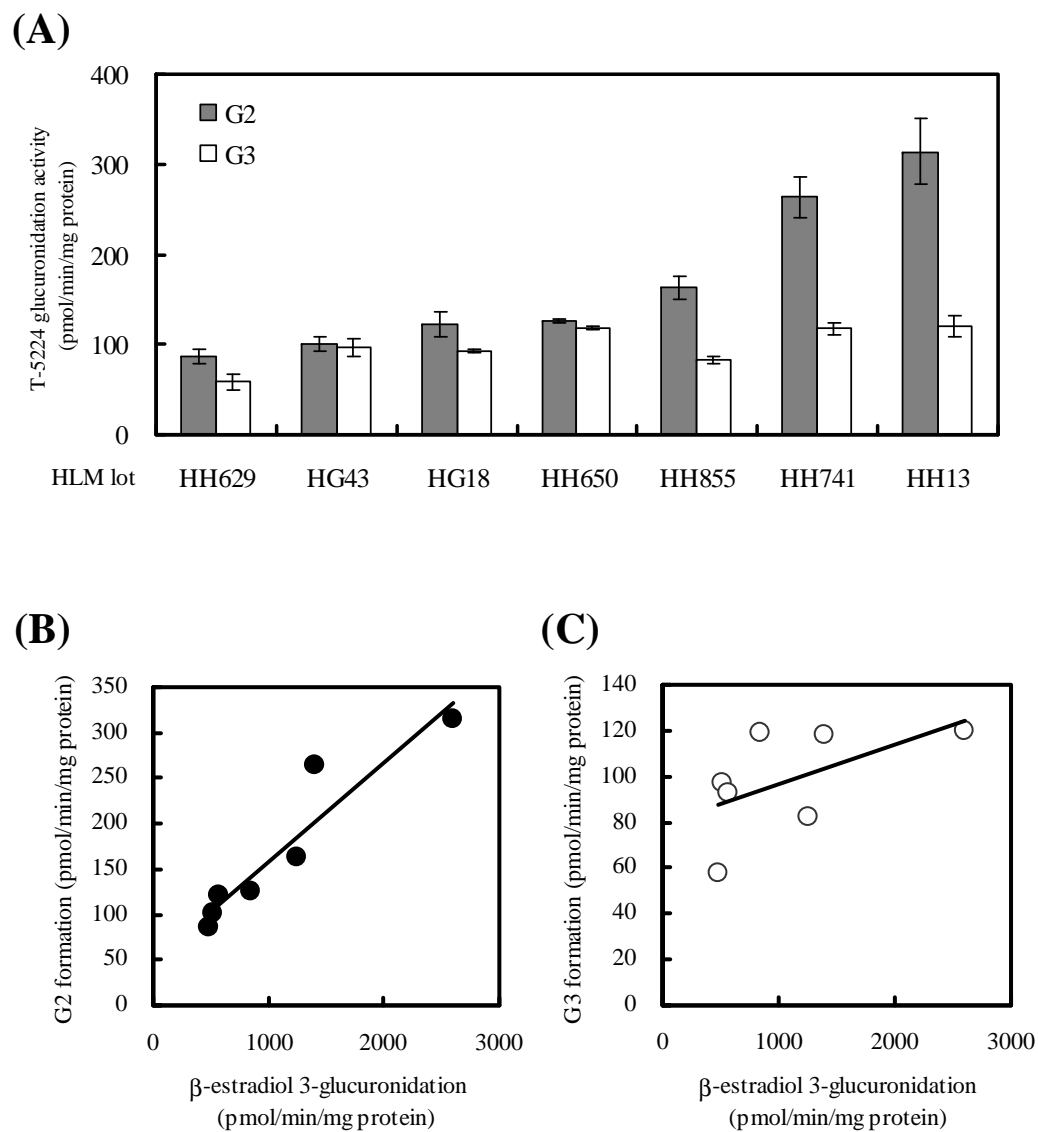
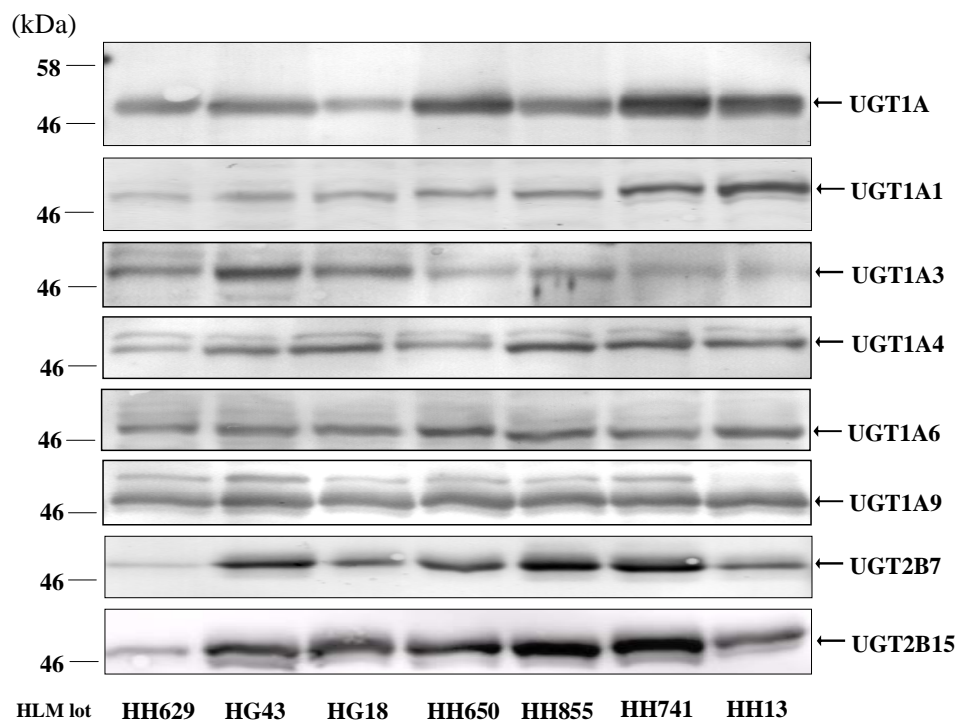
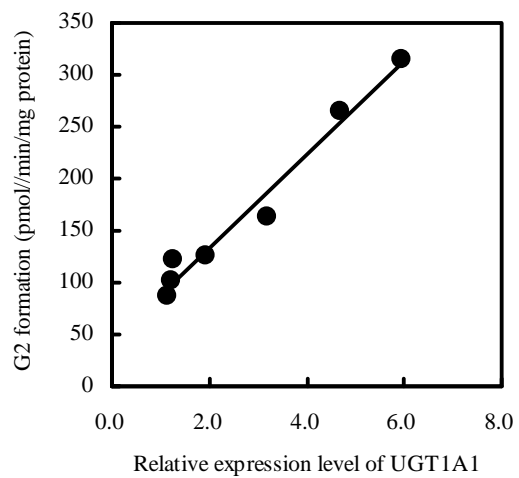


# Fig. 9

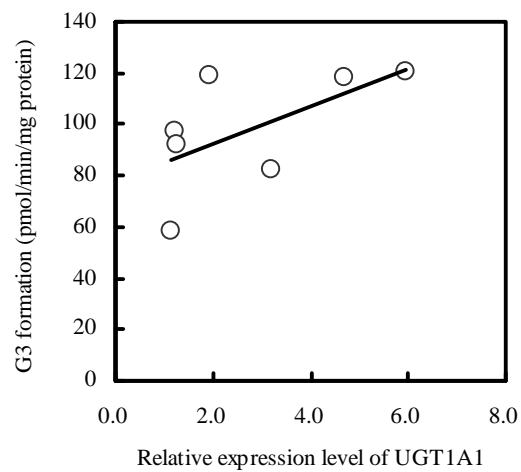
(A)



(B)



(C)



## Supplemental Data

Metabolism of the c-Fos/activator protein-1 inhibitor T-5224 by multiple human UGT isoforms

Shinsuke Uchihashi, Hiroyuki Fukumoto, Makoto Onoda, Hiroyoshi Hayakawa, Shin-ichi Ikushiro, Toshiyuki Sakaki

### DRUG METABOLISM AND DISPOSITION

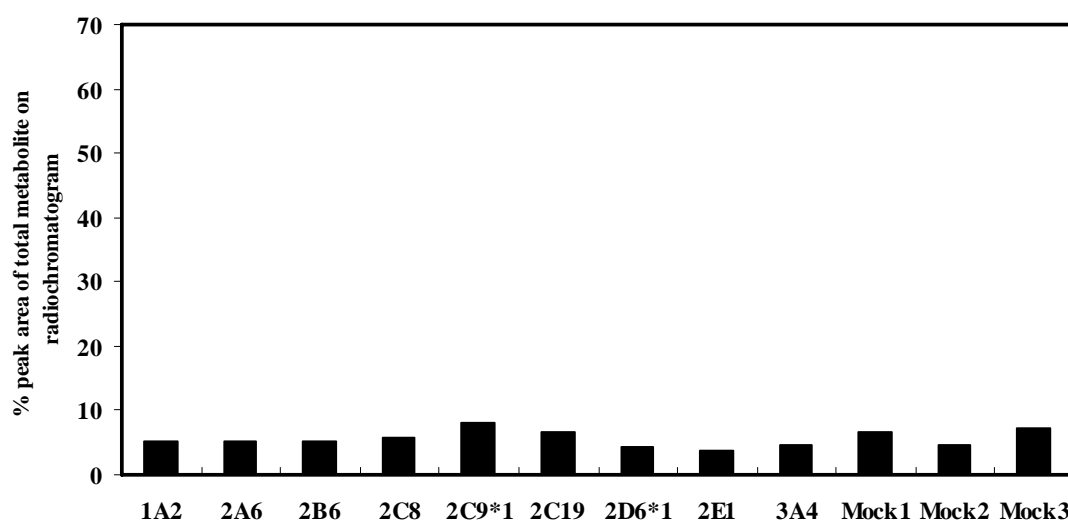


**Fig. s1** Ratio of T-5224 metabolites generated by recombinant human cytochrome P450.  $^{14}\text{C}$ -T-5224 (2  $\mu\text{M}$ ) was incubated for 30 min at 37°C and radioactive peak of metabolites were detected. Mock 1; control for CYP1A2 and CYP2D6\*1. Mock 2; control for CYP2B6, CYP2C8, CYP2C19, CYP2E1 and CYP3A4. Mock 3; control for 2A6 and 2C9\*1.

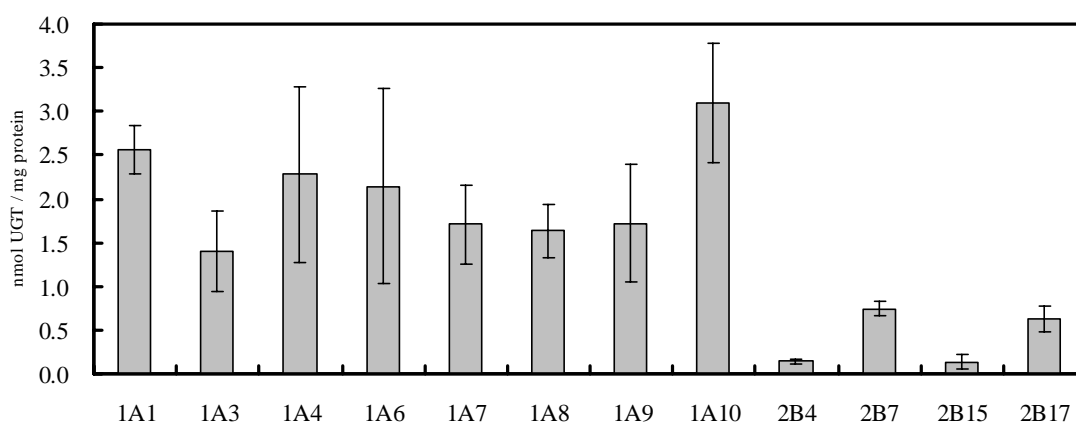
## Supplemental Data

Metabolism of the c-Fos/activator protein-1 inhibitor T-5224 by multiple human UGT isoforms

Shinsuke Uchihashi, Hiroyuki Fukumoto, Makoto Onoda, Hiroyoshi Hayakawa, Shin-ichi Ikushiro, Toshiyuki Sakaki

DRUG METABOLISM AND DISPOSITION

(A)



(B)

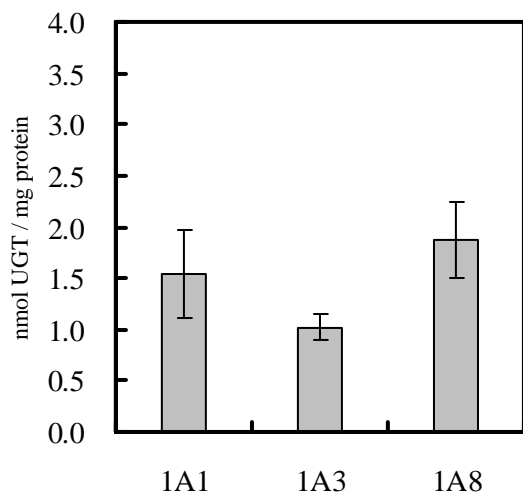


**Fig. s2** UGT contents in recombinant human UGT microsomes used in screening study (A), and kinetics study and inhibition study (B). UGT contents were estimated by quantitative immunoblot analysis using anti-UGT1A or anti-UGT2B antibodies. Known-concentration UGT1A1

## Supplemental Data

or UGT2B4 was used as standards. Values are represented as mean  $\pm$  standard error (n = 3 to 6).

## Supplemental Data

Metabolism of the c-Fos/activator protein-1 inhibitor T-5224 by multiple human UGT isoforms

Shinsuke Uchihashi, Hiroyuki Fukumoto, Makoto Onoda, Hiroyoshi Hayakawa, Shin-ichi Ikushiro, Toshiyuki Sakaki

DRUG METABOLISM AND DISPOSITION

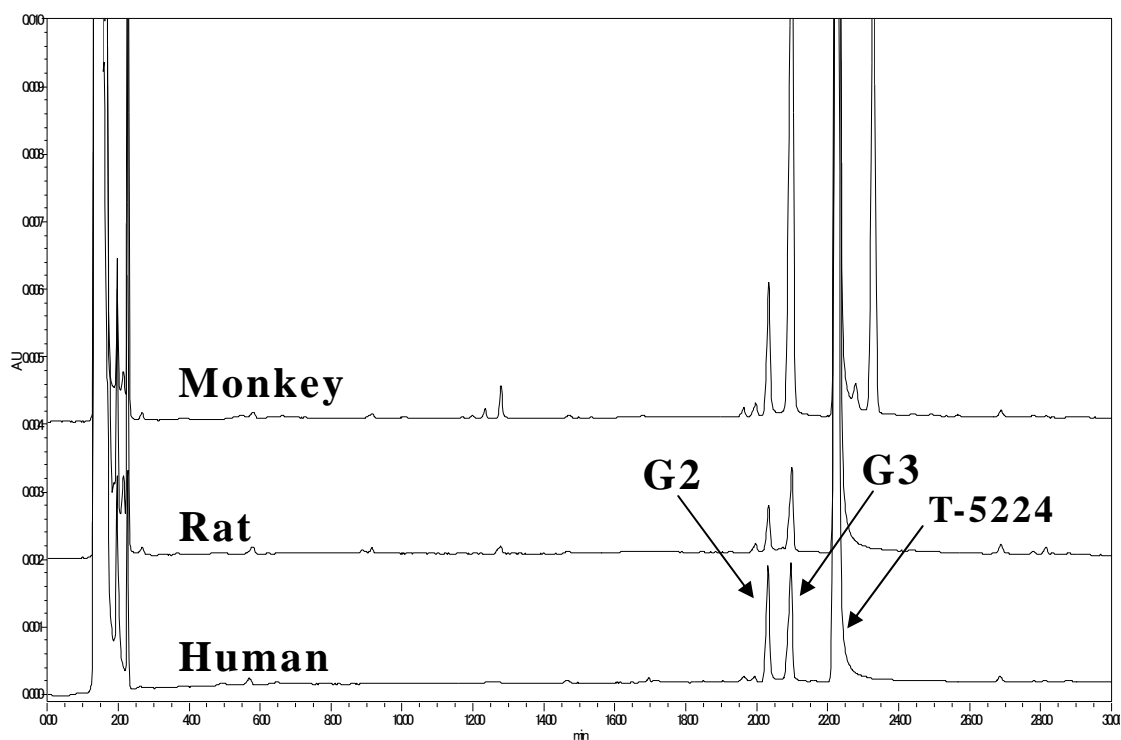


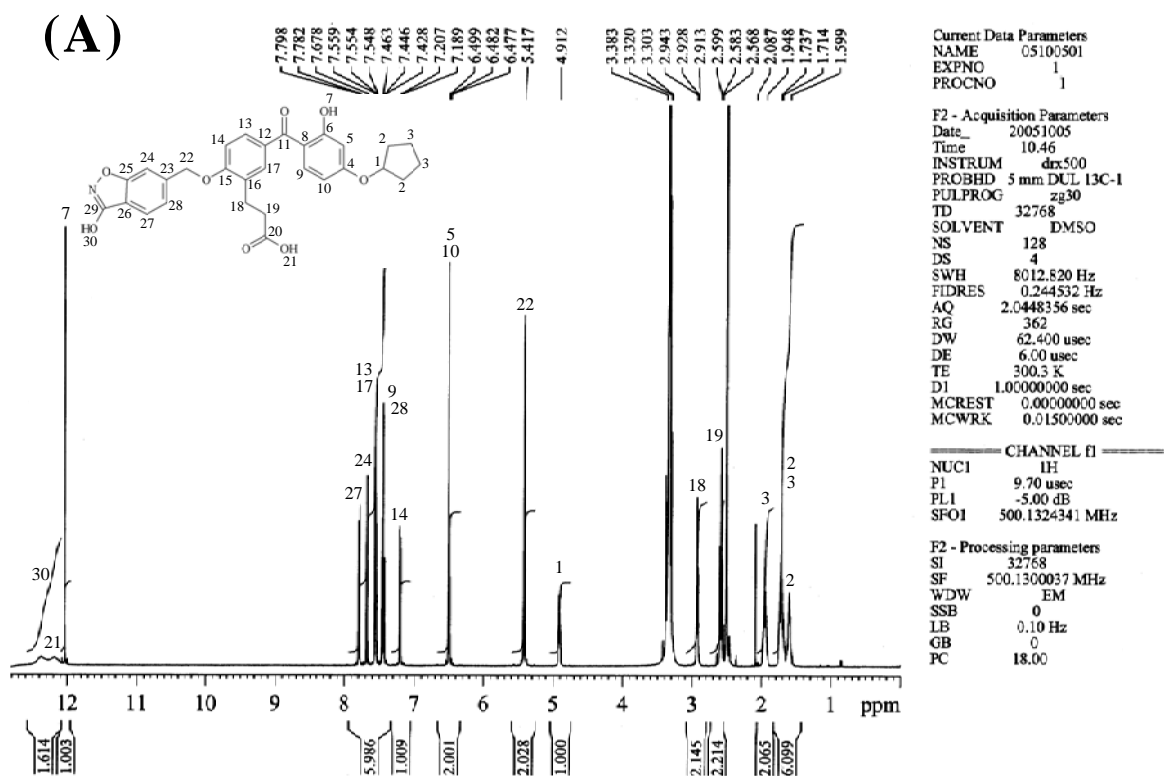
**Fig. s3** HPLC profiles of T-5224 and its glucuronides in liver microsomes from human, rat and monkey. T-5224 (10  $\mu$ M) was incubated at 37°C with UDP-glucuronic acid for 10 min in pooled liver microsomes.

## Supplemental Data

Metabolism of the c-Fos/activator protein-1 inhibitor T-5224 by multiple human UGT isoforms

Shinsuke Uchihashi, Hiroyuki Fukumoto, Makoto Onoda, Hiroyoshi Hayakawa, Shin-ichi Ikushiro, Toshiyuki Sakaki

DRUG METABOLISM AND DISPOSITION



# Supplemental Data

(Continued)

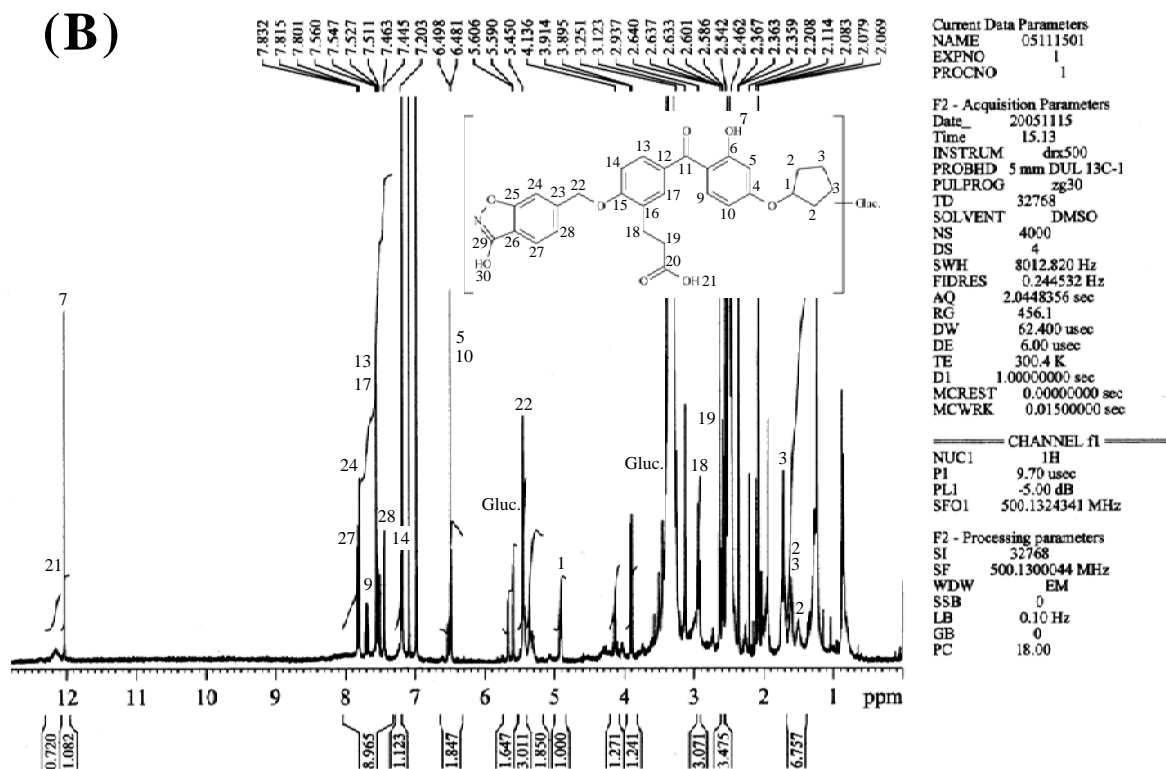


**Fig. s4**  $^1\text{H-NMR}$  spectrum of T-5224 (A) and hydroxyl-glucuronide isolated from monkey bile (B).